

# A QUANTIFICATION OF PEAK FORCE IN A SWITCHING CONTROLLED IMPACT OPERATION

Djitt Laowattana

Panrasee Ritthipravat

Center of Operation for Field Robotics Development (FIBO)

King Mongkut's University of Technology Thonburi

91 Suksawas road Tongkrui Bangkok Thailand

Phone (662)470-9339, Fax. (662)470-9111 e-mail: s070406@cc.kmutt.ac.th

## Abstract

Contact transition must be thoroughly understood and controlled such that industrial robots can effectively perform an impact force operation. There are three different stages in controlling robots while interacting with environment, i.e. pre-collision, impact and post-collision stages. In this paper, we present an analytical derivation of an impact control, together with its experimental results using a switching method. We quantify peak forces during impact based on parameters during the pre-collision stage. Such a quantification is verified by experiments on our one d.o.f manipulator.

## Nomenclatures:

- m : Mass.
- k : Stiffness.
- b : Damping.
- e : Coefficient of restitution.
- x : Displacement.
- $\dot{x}$  : Velocity.
- $P_n$  : Normal impulse.
- F : Force.

## Subscriptions:

- s : Sensor.
- r : Robot.
- rf : Flexible part.
- k : Contact.
- p : Peak.
- a : Actuator.

## 1. Introduction

In general, industrial robots operate under position control. Applications of this free motion are spot-welding, pick and place etc. To increase robot capability in force-constrained tasks, we must understand the physical interaction occurring between end-effectors and environment. Several researchers have been contributing to such understanding. Eppinger [1] studied stability limitations on force control schemes and integrated an effect of compliance into robotic force operation. Richard Volpe and Pradeep Khosla [10,11,13] analyzed and provided experimental verification of the fourth order model of a force

controlled plant. Different system parameters lead to different predicted behavior for force controllers. Their experimental results were compared to basic strategies that had been proposed for force control of robotic manipulators, i.e. proportional controller with a feedforward component, integral, filtered feedback proportional-derivative controller and a second order low pass filter. The force trajectory tracking was found the best under an integral gain explicit force control. The PD force control and damping strategies should not be implemented to enhance stability, especially when in contact with the environment since it is impossible to obtain a true derivative. Nitish Mandal and Shahram Payandeh [2] proposed an explicit force control scheme of a manipulator in contacting stiff environment with compliance. Shahram Payandeh and Andrew A. Goldenberg [14] presented a robust force controller for a manipulator contacting with a rigid environment based on a general theory of servomechanism problems. The contact problem is one of the most crucial problems in constrained tasks. This problem introduces residual impact forces usually occurring while end-effectors come into contact with environment. Contact problems have been analyzed in order to achieve smooth stable transition between free motion and force control, avoiding large force spikes. James M. Hyde and Mark R. Cutkosky [3] proposed a new approach on input commands preshaping to suppress vibration. This method removed most of residual vibration, but some oscillation still remained. G. T. Marth, T. J. Tarn and A. K. Bejezy [4] introduced a nonlinear feedback based algorithm which was combined with an explicit force control. In this work, a switching control is used and stability analysis of phase transition was described. Yunying Wu, Tzyh-Jong Tarn and Ning Xi [5] proposed an impact control under and a positive acceleration feedback control scheme, by using the feedback linearization and a decoupling technique. Miomir Vukobratovic [6] presented an overview of contact control. Eunjeong Lee, Kenneth A. Loparo, Roger D. Quinn [7] introduced a robust impedance/time-delay control algorithm with a negative force feedback to absorb impact force control by using a bang-bang control. James K. Mills [8] studied an open loop control to control over generalized contact forces and positions

while a robot was contacting tasks. This method cannot provide a desired performance of a closed-loop force control. In addition, it works well only under low acceleration and velocity conditions. Richard Volpe and Pradeep Khosla [9] presented a new impact control strategy based on a proportional gain explicit force controller with feedforward signals and negative gains. This controller is equivalent to the second order impedance control with a large target mass. This control gain, however, cannot be used to track inputs. They did not concern heavily on impact components in their plant modeling. James K. Mills [12] investigated stability and control of robotic manipulators during a transition from noncontacting to contacting modes, or vice versa. No dynamic model of manipulators during collision was analyzed. He assumed that the surface of the work environment deformed very rapidly, as collision occurs, with a much shorter time constant than the environment dynamics. Two separate control strategies were designed. The first control was synthesized to stabilize manipulators during free motion, the second was designed for contact motion. The control input was switched discontinuously depending on contacting states. The concept of generalized dynamical systems forms a very powerful tool with which the stability of a certain dynamic system is analyzed.

As indicated above, most of previous works, were devoted to impact modeling based on either deformation theory or conservation of momentum. In our work, we are interested in using an impact model based on the momentum theory but focus on triangular pulse shape. The peak forces during impact are quantified and experimented on our one d.o.f manipulator.

## 2. Mathematical Modeling of an Impact

In modeling a robot arm, we concern the effect of flexibility resulting from noncollocation of actuators and sensors. By adding masses, springs, dampers between actuators and sensors, this model can represent the effect of flexibility. Such flexibility introduces complex poles into its transfer function that often has very low damping and creates difficulties in providing a fast, stable system. We will use this model to study our impact problem. To understand fundamental behavior of this impact problem, we designed and built a testbed of one d.o.f robot arm as shown in Fig. 1, together with the development of a control algorithm. Fig. 2 graphically depicts a lumped mass model of our testbed. The robot arm itself is represented by two masses,  $m_{r1}$  and  $m_{r2}$ , and flexibility between them is given by stiffness  $k_{rf}$

and a damping  $b_{rf}$ . The damping to ground of such a robot arm is given by  $b_r$ . We will model a force sensor with stiffness  $k_s$  and damping  $b_s$ . In reality,  $b_s$  is relatively much less than  $k_s$ . These parameters are physically measured and summarized in Table 1.

$m_{r1}$	2.1155 kg.	$k_{rf}$	1577.315N/m.
$m_{r2}$	1.8105 kg.	$k_s$	908.9052N/m.
$b_r$	100 Ns/m	$b_{rf}$	28 Ns/m.
$b_s$	0 Ns/m	e	0.9

Table 1 System parameters

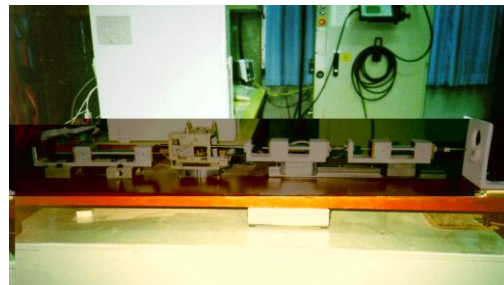


Fig. 1 A testbed of our one d.o.f robot arm

There are three different stages in controlling such an impact, i.e. pre-collision, impact and post-collision stages. Fig. 2 also represents a lumped mass model for pre-collision stage without kinematic constraint. Impact and post-collision stages with kinematic constraint are shown in Fig. 3. Kinematic constraints, similar to motion constraints, prohibit displacement in certain directions, resulting in reduction of d.o.f.

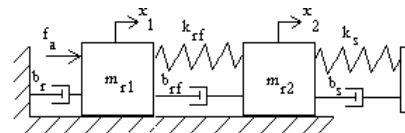


Fig. 2 A lumped mass one DOF robot model for pre-collision stage.

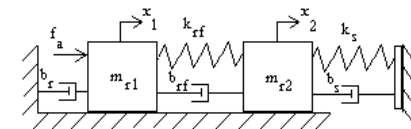


Fig. 3 A lumped mass one DOF robot model with kinematic constraint.

From Fig. 2, We represent the displacement of mass  $m_{r1}$  and  $m_{r2}$  by  $x_1$  and  $x_2$  respectively. Using the second law of Newton, equations of motion are

$$m_{r1}\ddot{x}_1 = f_a + k_{rf}(x_2 - x_1) + b_{rf}(\dot{x}_2 - \dot{x}_1) - b_r\dot{x}_1, \quad (1)$$

$$m_{r2}\ddot{x}_2 = -k_{rf}(x_2 - x_1) - b_{rf}(\dot{x}_2 - \dot{x}_1). \quad (2)$$

When the robot comes into contact with the environment as shown in Fig.3, the equations of motion are the one similar to equation (1) and

$$m_{r2}\ddot{x}_2 = -k_{rf}(x_2 - x_1) - b_{rf}(\dot{x}_2 - \dot{x}_1) - k_s x_2 - b_s \dot{x}_2. \quad (3)$$

By the nature of mechanical impact processes, interaction forces are residential during a time interval of contact  $\tau_1$  to  $\tau_2$ . Fig. 4 shows a typical force-time pulse. It is frequently convenient to use an ideal triangular force instead of the actual impulse, as shown dashed in Fig. 4 with a dashed line.

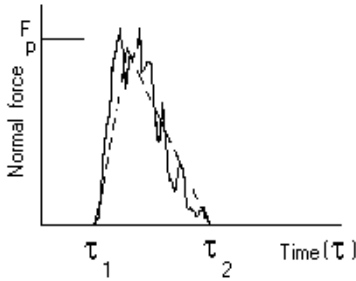


Fig. 4 A typical normal force variation for an impact.

We introduce an impulse model as

$$P_n = m_{r2}(\dot{x}_2' - \dot{x}_2) = -\frac{1}{2}F_p(\tau_2 - \tau_1), \quad (4)$$

where  $P_n$  represents the normal impulse, defined as an area under the force-time curve.  $F_p$  is a normal peak force or an impulse force of which minus sign indicates direction of impulse force.

$\dot{x}_2'$  is the velocity after collision. Upon impact, we could determine amount of energy being dissipated to environment by the coefficient of restitution,  $e$ . This coefficient is defined as an absolute ratio between velocities after collision,  $\dot{x}_2'$  and before collision,  $\dot{x}_2$ .

$$\dot{x}_2' = -e\dot{x}_2. \quad (5)$$

Manipulating equations (4) and (5), we obtain

$$P_n = m_{r2}(\dot{x}_2' - \dot{x}_2) = -\frac{1}{2}F_p(\tau_2 - \tau_1) = -m_{r2}(e+1)\dot{x}_2, \quad (6)$$

leading to

$$F_p = \frac{2m_{r2}(e+1)\dot{x}_2}{(\tau_2 - \tau_1)}. \quad (7)$$

According to equation (7), we define  $(\tau_2 - \tau_1)$  as period of impact,  $\delta$  which makes high forces when it is small. We represent the dynamics model in three stages as pre-collision, impact and post-collision stages. We will discuss each stage as follow.

**2.1 Pre-Collision Stage :** According to equation (1) and (2), we derive its transfer function of this plant as.

$$\frac{X_1(s)}{F_a(s)} = \frac{m_{r2}s^2 + b_{rf}s + k_{rf}}{(m_{r1}s^2 + (b_r + b_{rf})s + k_{rf})(m_{r2}s^2 + b_{rf}s + k_{rf}) - (b_{rf}s + k_{rf})^2}, \quad (8)$$

$$\frac{X_2(s)}{F_a(s)} = \frac{b_{rf}s + k_{rf}}{(m_{r1}s^2 + (b_r + b_{rf})s + k_{rf})(m_{r2}s^2 + b_{rf}s + k_{rf}) - (b_{rf}s + k_{rf})^2}. \quad (9)$$

We plot a root locus based on parameter in table 1. Its root locus in z-plane is shown in Fig. 5 indicating four poles at 1, 0.91560.12i, 0.803. Because of a pole at 1, the system is of type 1, thus a P or PD-controller would be adequate for this system.

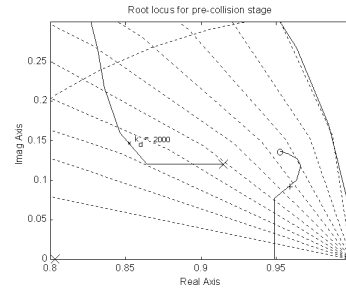


Fig. 5 Root locus of the pre-collision plant.

**2.2 Impact Stage:** In this stage, the robot arm is constrained with an environment. Equations of motion are similar to equations (1) and (3). The impulse model is now integrated as indicated in equation (7). We obtain the transfer function of plant as equation (8) and

$$X_2(s) = \frac{(b_{rf}s + k_{rf})X_1(s)}{(m_{r2}s^2 + (b_{rf} + b_s)s + (k_{rf} + k_s))}, \quad (10)$$

$$X_2(s) = \frac{F_p(s)\delta}{2m_{r2}(e+1)s}, \quad (11)$$

leading to a relation between the actuator force,  $F_a(s)$  and the peak force,  $F_p(s)$  from equations (8), (10) and (11) as

$$F_p(s) = \frac{F_a(s)}{A} + \frac{B}{A}. \quad (12)$$

Where

$$A = \left\{ \frac{1}{2} \delta [(m_{r1} m_{r2}) s^4 + (m_{r1} b_{rf} + m_{r2} (b_r + b_{rf})) s^3 + m_{r1} (k_{rf} + k_s) s^2 + (m_{r2} k_{rf} + b_r b_{rf}) s^2 + (b_r (k_{rf} + k_s) + b_{rf} k_s) s + k_{rf} k_s] \right\} / ((b_{rf} s + k_{rf}) (m_{r2} (e+1) s)),$$

and

$$B = \{ (m_{r1} m_{r2} \ddot{x}_2(\tau_1)) s^3 + (m_{r2} (b_r + b_{rf}) \dot{x}_2(\tau_1) - m_{r1} (k_{rf} + k_s) x_2(\tau_1)) s^2 + (m_{r1} k_{rf} \dot{x}_1(\tau_1) + m_{r1} b_{rf} \dot{x}_1(\tau_1)) s^2 + (m_{r2} k_{rf} \dot{x}_2(\tau_1) + (-b_r (k_s + k_{rf}) - b_{rf} k_s) x_2(\tau_1)) s + (m_{r1} k_{rf} \dot{x}_1(\tau_1) + b_r k_{rf} x_1(\tau_1)) s - k_{rf} k_s x_1(\tau_1) \} / (b_{rf} s + k_{rf})$$

The terms B is composed of initial term  $x_1(\tau_1)$ ,  $x_2(\tau_1)$ ,  $\dot{x}_1(\tau_1)$  and  $\dot{x}_2(\tau_1)$  which represent position and velocity of mass  $m_{r1}$  and  $m_{r2}$  before impact respectively. We can determine these values from responses of the pre-collision stage.

**2.3 Post-Collision Stage:** The equations of motion of our testbed with kinematic constraint are shown in equations (1) and (3) further derived to obtain transfer functions for this stage as

$$\frac{X_1(s)}{F_s(s)} = \frac{m_{r2} s^2 + b_{rf} s + k_{rf}}{(m_{r1} s^2 + (b_r + b_{rf}) s + k_{rf}) (m_{r2} s^2 + (b_{rf} + b_s) s + (k_{rf} + k_s)) - (b_{rf} s + k_{rf})^2} \quad (13)$$

$$\frac{F_s(s)}{F_s(s)} = \frac{k_s X_2(s)}{F_s(s)} = \frac{k_s (b_{rf} s + k_{rf})}{(m_{r1} s^2 + (b_r + b_{rf}) s + k_{rf}) (m_{r2} s^2 + (b_{rf} + b_s) s + (k_{rf} + k_s)) - (b_{rf} s + k_{rf})^2} \quad (14)$$

Our particular goal is to achieve smooth, stable transitions during contact states. In the next section, we use a switching method to switch from one stage to another. If the manipulator and environment are not in contact indicating that no interactive force is sensed, i.e.  $F_s = 0$ . When the manipulator and the environment are in contact, then  $F_s$  is larger than zero. Such a pre-collision stage is switched to the impact stage. At the end of the impact, the end-effector reacts at constant force, the impact stage is switched to post-collision stage. The value of  $F_s$  is then checked as conditions for switching.

### 3. Switching Control Algorithm.

Since we separate different stages in the impact process, we propose a switching method for controlling these three stages as follow.

### 3.1 Pre-Collision Stage

In this stage, a position control is designed based on a proportional control. According to Fig. 5, we select  $k_p = 2000$ , which has damping factor = 0.6. We can determine a position and a velocity of mass  $m_{r1}$  and  $m_{r2}$  while the end-effector collides with a workpiece as shown in Fig. 6. We set a position of  $m_{r1}$  to be 0.001 m. leading to a position of  $m_{r2}$ , velocity of  $m_{r1}$  and velocity of  $m_{r2}$ , while end-effector collide workpiece, as 0.001 m., 0.007 m/sec. and 0.013 m./sec respectively. These values affect impulse response to be discussed in 3.2.

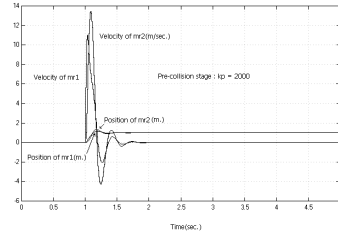


Fig. 6 Position and velocity of mass  $m_{r1}$  and  $m_{r2}$

### 3.2 Impact Stage

Refer to equation (12), we obtain a transfer function of system as  $\frac{1}{A}$ . We design a PD-controller in the z-plane using the root locus method. By connecting the controller with the system, we can plot a root locus by letting  $k_d = 0$  and determine  $k_p$  based on Fig. 7. We select  $k_p = -0.3$  which has a damping factor about 0.35 and plot a root locus of system as shown in Fig. 8. According to Fig. 8, we select  $k_d = 0.1$  which has a damping factor as highest as we can obtain. We test our system through a impulse function. We obtain impulse response as shown in Fig. 9. The same design is simulated for Fig. 10 which has  $k_p = 0.3$  and  $k_d = 0.1$

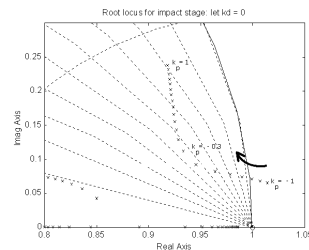


Fig. 7 Root locus for impact stage ( $k_d = 0$ ).

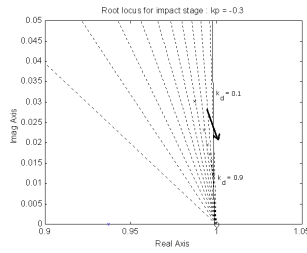


Fig. 8 Root locus for impact stage ( $k_p = -0.3$ )

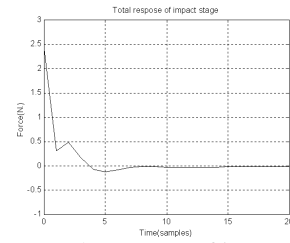


Fig. 12 Total response of impact stage.

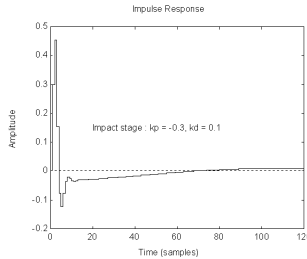


Fig. 9 Impact stage ( $k_p = -0.3$  and  $k_d = 0.1$ )

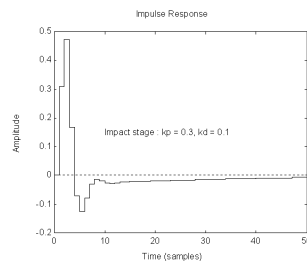


Fig.10 Impact stage ( $k_p = 0.3$  and  $k_d = 0.1$ )

Refer to equation (12), this impulse response will add an initial condition term  $\frac{B}{A}$  in order to obtain the actual  $F_p$ . As discussed in section 3.1, we plot the force resulting from initial terms for impact stage in Fig. 11. The total force during the impact stage is determined by superpositioning results by the impulse response and initial terms in equation (12). This superposition is shown in Fig. 12.

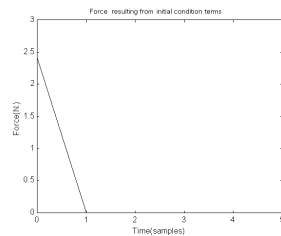


Fig. 11 Force resulting from initial term for impact stage

As shown in Fig. 12, the initial affects high residential values in the impact response. Thus we should limit force resulting from initial terms by properly bounded initial terms. In limiting initial terms such as velocity of  $m_{r1}$  and  $m_{r2}$ , we may put a brake on the end-effector before it collides with a workpiece. Another way is to actively specify the initial terms through corresponding controller.

### 3.3 Post-Collision Stage

At the end of impact stage, a force control is designed based on a PID-concept. To obtain a continuity in switching, rise time of this response must be as fast as possible within actuator saturation limit. We select  $k_p = 2$ ,  $k_i = 10$  and  $k_d = 0.1$  in a simulation to a step response. The result is shown in Fig. 13.

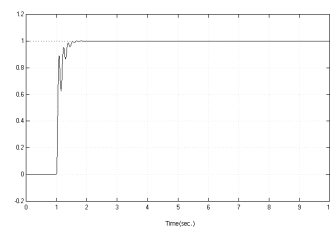


Fig. 13 Step response of pre-collision stage

## 4. Experimental Results

We implement our impact algorithm on testbed of 1 d.o.f robot arm. We encounter inaccuracy of the parameters leading inaccurate gains during simulation. Fine tuning is performed in order to get the best perform. We set force reference at 3 N. Sampling period is 0.005 sec. From our experimental results, we accomplish response the same as our simulation. We show our experimental results in Fig. 14, which under with  $k_p = 2000$  in Pre-collision stage,  $k_p = -3$  and  $k_d = 0.2$  in impact stage,  $k_p = 3$ ,  $k_d = 0.2$  and  $k_i = 7$  in post-collision stage. In the Fig. 15 which control with  $k_p = 2000$  in Pre-collision stage,  $k_p = 3$  and  $k_d = 0.2$  in

impact stage,  $k_p=3$ ,  $k_d=0.2$  and  $k_i=7$  in post-collision stage. These results show the range of impact stage gain same as our simulation.

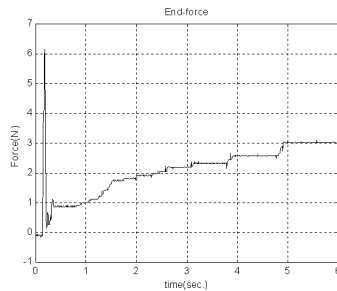


Fig. 14 Experimental Result on Force control  
( $k_p=3$  and  $k_d=0.2$  for impact stage)

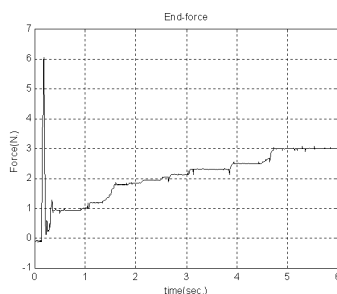


Fig. 15 Experimental Result on Force control  
( $k_p=3$  and  $k_d=0.2$  for impact stage)

## 5. Discussion and Conclusion

In this paper, impulse equation focusing on triangular pulse shape is integrated into an impact modeling. From the experimental results, when collision occurs, the impulse force decreases rapidly then it comes to the end of transition stage. At this post-collision stage, the controller try to track the reference force. Although the technique in bounding the initial terms only gives the threshold of the impact force and do not suppress all impulse forces, we can dissipate energy of impact to robot arm. After switching to the impact stage, a PD-controller provides responses similar to our simulation as shown in Fig. 12 and initial terms of an impact modeling cause a first peak force. This indicates that our impact modeling is reliable. We obtain a relation of these initial terms to peak forces. Thus in implementing on real industrial robots, we can optimize peak force and approaching terms to provide this peak force in a limit of acceptable ranges. Such ranges can be considered as specifications in designing controllers for the pre-collision stage.

## 6. Acknowledgement

The funding for this research is supported from the National Science and Technology Development Agency (NSTDA). Program number CO-B-06-44-20-101. The authors highly appreciate such a research funding.

## 7. Reference

- [1] Steven D. Eppinger, "Modeling Robot Dynamic Performance for Endpoint Force Control", technical report, AI Lab, MIT. August 1988.
- [2] Nitish Mandal and Shahram Payandeh, "Force Control Strategies for Compliant and Stiff Contact : Experimental Study", IEEE 1994.
- [3] James M. Hyde and Mark R. Cutkosky, "Contact Transition Control : An Experimental Study", IEEE 1993.
- [4] Yunying Wu, Tzyh-Jong Tarn and Ning Xi, "Force and Transition Control with Environmental Uncertainties", IEEE international conference on robotics and automation 1995.
- [5] G. T. Marth, T. J. Tarn and A. K. Bejczy, "Stable Phase Transition Control for Robot Arm Motion", IEEE 1993.
- [6] Miodir Vukobratovi'c, "Contact Control Concepts in Manipulation Robotics-An Overview", IEEE 1994.
- [7] Eunjeong Lee, Kenneth A. Loparo and Roger D. Quinn, "A Nonlinear Bang-Bang Impact Force Control", IEEE conference on decision and control.
- [8] James K. Mills, "Robotic Manipulator Control of Generalized Contact Force and Position", IEEE Transactions on systems, Vol.24, No. 3, March 1994
- [9] Richard Volpe and Pradeep Khosla, "Experimental Verification of a Strategy for Impact Control" IEEE International Conference on Robotics and Automation, April 1991
- [10] Richard Volpe and Pradeep Khosla, "Theoretical Analysis and Experimental Verification of a Manipulator / Sensor / Environment Model for Force Control", IEEE 1990.
- [11] Richard Volpe and Pradeep Khosla, "Analysis and Experimental Verification of a Forth Order Plant Model for Manipulator Force Control", IEEE Robotics & Automation Magazine.
- [12] James K. Mills, "Manipulator Transition To and From Contact Tasks: A Discontinuous Control Approach", IEEE 1990.
- [13] Richard Volpe and Pradeep Khosla, "An Experimental Evaluation and Comparison of Explicit

Force Control Strategies for Robotic Manipulators”, Proceeding of the 1992 IEEE, International Conference on Robotics and Automation.

[14] Shahram Payandeh and Andrew A. Goldenberg, “A Robust Force Controller: Theory and Experiments”, Proceedings of the 1991 IEEE International Conference on Robotics and Automation.

[15] Raymond M. Brach, “Mechanical Impact Dynamics: Rigid body collisions”, 1991 John Wiley & Sons, New York.

[16] Benjamin C. Kuo, “Automatic Control Systems”, Prentice Hall, 1995.

[17] Benjamin C. Kuo, “Digital Control Systems”, Saunders College Publishing, 1992.

### **Dr. Djitt Laowattana.**

Dr. Laowattana’s research is primarily in fundamental areas of robotic dexterity, design for manufacturing / assembly and nonlinear control theory. He was awarded an honor with his B.Eng. from King Mongkut’s Institute of Technology Thonburi (KMUTT). Under the Monbusho Program, he carried out research in robot force control at Kyoto University, Japan during 1986-1988. He received Ph.D. in 1994 from Carnegie Mellon University, USA under financial support from the Fullbright Fellowship Program and the AT&T Advanced Research Program. In 1996, he obtained a certificate in Management of Technology from Massachusetts Institute of Technology USA. He holds two US patents and has founded the Center of Operation for Field Robotics Development (FIBO) at KMUTT, Thailand, where he is serving as a research scientist.



### **Ms. Panrasee Ritthipravat.**

Ms. Ritthipravat graduated from King Mongkut’s Institute of Technology Thonburi (KMUTT) with a Bachelor Degree in Mechanical Engineering. The fruit-milling machine was her thesis. Currently she is a graduate student at KMUTT, working on robot force control. Her research is under a financial support from the National Science and Technology Development Agency (NSTDA). She is a researcher assistant at Center of Operation for Field Robotics Development (FIBO) at KMUTT, Thailand.

